Assessment of the wind power generation uncertainty on the steady-state operation of electric power systems

Uriel F. Sandoval Pérez, Claudio R. Fuerte-Esquivel

Ver material suplementario

Publicado en línea, enero de 2022

Envíe su artículo a esta revista

Assessment of the wind power generation uncertainty on the steady-state operation of electric power systems

Uriel F. Sandoval Pérez *, Claudio R. Fuerte-Esquivel

Universidad Michoacana de San Nicolás de Hidalgo, Facultad de Ingeniería Eléctrica

Resumen

Hoy en día, la integración a gran escala de sistemas de conversión de energía eólica en las redes de energía eléctrica es una de las opciones más efectivas y prácticas para generar electricidad a partir de fuentes renovables. Sin embargo, el aumento en el desarrollo de la energía eólica hace que el funcionamiento de los sistemas de energía eléctrica se vuelvan más dependientes y vulnerables a las variaciones en la velocidad del viento. En este contexto, es necesario realizar estudios probabilísticos de flujo de potencia (PPF) para mantener la integridad del sistema frente a la generación estocástica de energía eólica. Este documento describe e implementa un método de flujo de energía que considera las incertidumbres que surgen del comportamiento de la generación eólica. Este enfoque PPF, basado en una técnica de estimación puntual, es validado frente a miles de simulaciones de Monte Carlo.

Palabras clave: energía eólica, redes de generación, probabilística de flujo de energía

Abstract

Nowadays, the large-scale integration of wind energy conversion systems in transmission networks is one of the most effective and practical options for generating electricity from renewable sources. However, the increase in wind energy penetration causes the operation of electrical power systems to become more dependent and vulnerable to variations in wind speed. Within this context, it is necessary to perform probabilistic power flow (PPF) studies to maintain system integrity in the face of stochastic wind power generation. This paper describes and implements a power flow method that considers the uncertainties that arise from wind generation behavior. This PPF approach, based on a point estimation technique, is validated against thousands of Monte Carlo simulations.

Keywords: Grid-connected wind generation, probabilistic power flow, point estimate method

Correspondencia de autor: sanurielf@gmail.com

Introduction

Electrical generation based on wind energy is a well-established conversion process in modern electrical power systems. Over the last couple of decades, regulatory incentives such as subsidies, stronger environmental initiatives, and significant advances in the design, construction and operation of wind generators, have played a major role in reducing the cost associated with this technology and the increase of maximum nameplate capacity of single wind turbines: from around 50 kW in the 1980s to nearly 6 MW found in current commercially available models (IRENA, 2019). This rapid technological development is leading to a rapid increase in the number of wind power facilities worldwide. According to the Global Wind Energy Council (GWEC) statistics, the wind industry had the best year in history in 2020 with a growth of 53% year-over-year, so that the new installations of 93 GW result in the total wind power capacity up to 743 GW (GWEC, 2021).

Over the years, the use of large-scale wind energy conversion systems (WECS) has become the most rapidly growing renewable energy source utilized in electricity generation all over the world, such that the power generated by wind turbines accounts for a considerable percentage of the total power production in different countries (GWEC, 2021). Even though wind energy is beneficial from an environmental standpoint, the complex task of achieving the controllability of an electric power system is even more demanding. Consequently, quantifying how the large-scale integration of wind generation affects the operation and control of electric networks requires special attention (Ahmed *et al.,* 2020).

Arguably, power flow analysis is the most frequently performed computational calculation for the steady-state analysis of power systems. Therefore, a suitable power flow algorithm considering steady-state models of wind generators is of paramount importance for the planning and operation of power networks. The earlier publications on this topic may be traced back to around 2000 (Feijoo and Cidras, 2000). Within this context, when the state variables of wind generators are not taken into account in the power flow formulation, these generators are modelled as conventional electric sources that inject a specified power into the transmission network, e.g., (Divya and Rao, 2006; Feijoo, 2009; Feijoo and Cidras, 2000; Padron and Lorenzo, 2010; Slootweg *et al.,* 2001). This approach is rather attractive because it is straightforward to consider wind-based power generation in existing power flow programs. Note also that this modelling approach is used in practice to assess the steady-state operating status of large-scale power systems.

The essential characteristic of wind energy exploitation is its intrinsic dependence on weather conditions. Consequently, the facilities devoted to produce electricity from the wind force constitute a new source of uncertainty in the power system operation and planning (Restrepo Hernandez, 2011). By using deterministic power flow routines, one must run them many times to encompass all, or at least the majority of, possible system states. In this context, the Monte Carlo (MC) simulation randomly generates values for uncertain input variables, and these values are then taken into account to solve a deterministic power flow. The main drawback of the MC method is the great number of simulations required to attain convergence. To reduce this computational burden, approximate methods can provide and approximate the statistical properties of random output variables without many simulations. Within these techniques, point estimate methods (PEMs)

stand out (Morales and Perez-Ruiz, 2007), where uncertainties associated with data employed in the power flow problem can be handled using the deterministic power flow formulation but with a much lower computational burden than the MC method.

In this case, the statistical properties of a random output variable are approximated by computing its statistical moments, i.e., mean, variance, skewness and kurtosis, as a function of a set of random input variables and the function relating both types of variables. The application of this method to the power flow problem has been reported in several works, where the uncertainties correspond to data associated with the nodal data and line parameters (Su, 2005), conventional power generation and load demands (Morales and Perez-Ruiz, 2007), load demands and wind power generation (Chen *et al.,* 2015; Gupta, 2016; Morales and Perez-Ruiz, 2007), wind farm power outputs (Ai *et al.,* 2012; Outcalt, 2009; Xiao *et al.,* 2017; Zhu *et al.,* 2020) as well as load demands and outages of generators (Mohammadi *et al.,* 2013). The PEM uses a specified number of estimated points that match the moments of the probability distribution function (PDF) of the random input variable. Hence, the accuracy of the PEMs depends on the number of points used to estimate the statistical moments of the random output variables. However, using many points increases the method's computational burden and the probability of calculating points outside the region where random input variables with large standard deviations are defined.

Based on the information mentioned above, this paper applies the five-point estimation method (5PEM) reported in (Gupta, 2016; Outcalt, 2009) to assess how the stochastic behavior of wind generation affects the steady-state operation of electric power systems. Within this context, the rest of the paper is structured as follows. For completeness, the power flow formulation to assess the steady-state operation of a power system is described in Section II, whereas the 5PEM is reported in Section III. Case studies associated with applying the developed PPF and comparing the numerical results against thousands of Monte Carlo simulations are presented in Section IV. This section also includes a flowchart of how the 5PEM and the power flow formulation are linked to formulating a probabilistic power flow (PPF) approach. Lastly, concluding remarks are given in Section V.

Conventional Power Flow Problem

Assuming that an electric power system is composed of a set of nodes $\mathcal{N} \coloneqq \{1, 2, \dots, N\}$ interconnected trough a set of transmission transmission elements, $\mathcal{T}e = \{1, 2, \dots, N_T\}$ the system's steady-state operation values of all nodal voltages, which can be grouped to form the vectors of voltage magnitudes $V = [V_1 \cdots V_N]^T \in \mathfrak{R}^N$ and voltage phase angles, $\theta = [\theta_1 \cdots \theta_N]^T \in \mathfrak{R}^N$ respectively. The superindex T denotes transpose. Thus, the power flow problem calculates voltage magnitudes and phase angles at each system's node based on a pair of equality constraints called power flow mismatch equations, formulated according to how the node operating conditions are defined (Acha *et al.,* 2004). The active and reactive power flow mismatch equations are given by (1) and (2), respectively, for nonregulated nodes $\mathcal{N}^{PQ} \subseteq \mathcal{N}$, referred to as *PQ* nodes:

$$\Delta P_i = P_i^{Gen} + P_{\omega,i}^{Gen} - P_i^{Load} - V_i \sum_{j \in \mathcal{N}} V_j \left[G_{ij} \cos\left(\theta_i - \theta_j\right) + B_{ij} \sin\left(\theta_i - \theta_j\right) \right] = 0, \ \forall i \in \mathcal{N}^{PQ} \ , (1)$$

$$\Delta Q_i = Q_i^{Gen} + Q_{\omega,i}^{Gen} - Q_i^{Load} - V_i \sum_{j \in \mathcal{N}} V_j \left[G_{ij} \sin\left(\theta_i - \theta_j\right) - B_{ij} \cos\left(\theta_i - \theta_j\right) \right] = 0, \ \forall i \in \mathcal{N}^{PQ}, (2)$$

where P_i^{Gen} and Q_i^{Gen} denote active and reactive powers, respectively, injected by a conventional generator into the *i*-th node, whereas P_i^{Load}

and Q_i^{Load} correspond to the active and reacitve powers demanded by loads embedded at the i-th node. Furthermore, *Gij* and *Bij* are the *ij*-th elements of the nodal conductance and susceptance matrices, respectively. Lastly, $P_{\omega,i}^{Gen}$ and $Q_{\omega,i}^{Gen}$ are active and reactive powers, respectively, injected by a wind farm into the i-th node. Note that these powers correspond to the random variables to be included in the power flow formulation.

The set of controlled voltage nodes $\mathcal{N}^{PV} \subseteq \mathcal{N}$, referred to as *PV* nodes, only consider the active power mismatch equation:

$$\Delta P_i = P_i^{Gen} + P_{\omega,i}^{Gen} - P_i^{Load} - V_i \sum_{i \in \mathcal{N}} V_j \left[G_{ij} \cos(\theta_i - \theta_j) + B_{ij} \sin(\theta_i - \theta_j) \right] = 0, \ \forall i \in \mathcal{N}^{PV} \quad (3)$$

On the other hand, $\Delta Q_i = 0, \forall i \in \mathcal{N}^{PV}$ as long as the reactive power output of the generator connected at the i-th node is within limits. If limits violation occurs, the PV node is transformed into a *PQ* node.

Lastly, the slack node does not have power flow mismatch equations because the voltage magnitude and phase angle values are known.

Since the set of power flow mismatch equation are nonlinear, the nodal volatges are obtained by iteratively solving the set of linearized algebraic equations (4), which results from expanding (1)-(3) into Taylor series and neglecting the higher-order terms, where k denotes the iteration number,

$$\underbrace{\begin{bmatrix} \Delta P \\ \Delta Q \end{bmatrix}^{(k)}}_{F(x^{(k-1)})} = - \underbrace{\begin{bmatrix} \frac{\partial \Delta P}{\partial \theta} & \frac{\partial \Delta P}{\partial V} V \\ \frac{\partial \Delta Q}{\partial \theta} & \frac{\partial \Delta Q}{\partial V} V \end{bmatrix}^{(k)}}_{J(x^{(k-1)})} \underbrace{\begin{bmatrix} \Delta \theta \\ \frac{\Delta V}{V} \end{bmatrix}^{(k)}}_{\Delta x^{(k)}} \quad (4)$$

In this case, $\Delta P \in \mathfrak{R}^{(N_{PQ}+N_{PV})}$, $\Delta Q \in \mathfrak{R}^{N_{PQ}}$, whereas, $\Delta \theta \in \mathfrak{R}^{(N_{PQ}+N_{PV})}$ and $\Delta V \in \mathfrak{R}^{N_{PQ}}$ represent the adjustments of nodal voltage magnitudes and phase angles, respectively. Lastly, $x = [\theta \ V] \in \mathfrak{R}^{(N_{PQ}+N_{PV})}$ and J is the Jacobian matrix.

The solution process of (4) for $\Delta X^{(k)} = [\Delta \theta \ \Delta V]^{(k)} \in \mathfrak{R}^{(N_{PQ}+N_{PV})}$ starts from flat voltages, and the nodal voltages are updated at each k-th iteration, i.e., $X^{(k+1)} = X^{(k)} + \Delta X^{(k)}$. This iterative solution continues until $\{\Delta P_i\}_{i=1}^{N_{PQ}}$ and $\{\Delta Q_i\}_{i=1}^{N_{PV}}$ are simultaneously less than a specified tolerance or the maximum number of iterations is achieved.
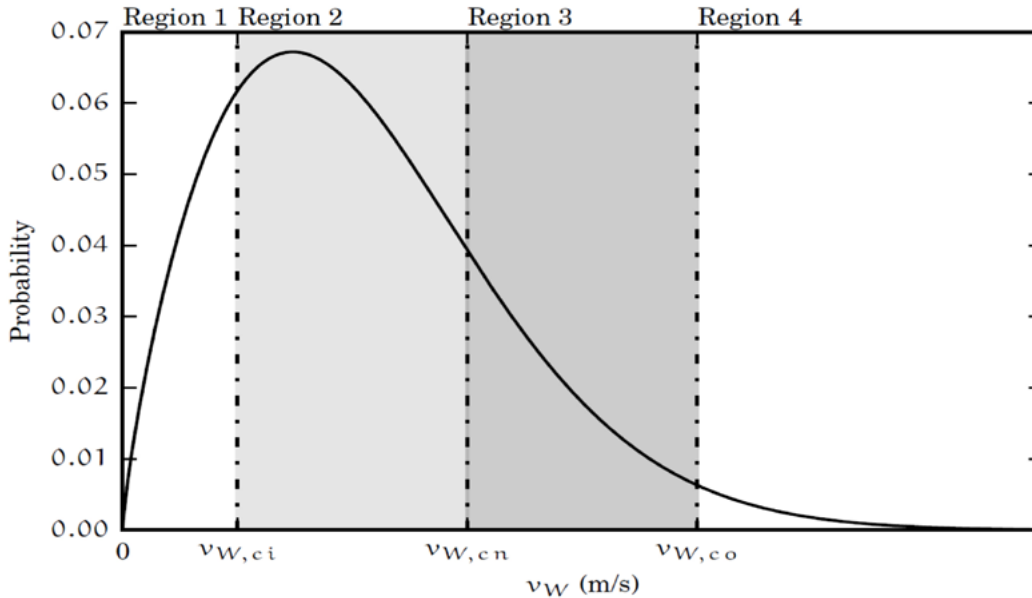

FIGURE 1. Weibull continuous PDF of wind speed.

Five-Point-Estimation

The direct approach for analyzing power flows under uncertainties is to use the well-known MC methods. These methods have a significant drawback: the better-desired accuracy, the more power flow simulations. In this context, it is necessary to have a tool that approaches the *exact* solution with less computational burden. (Outcalt, 2009) proposed the 5PEM, which discretizes wind power's continuous probability distribution function into five distinct points, each with its own probability.

This five-point distribution is calculated to have the same mean and standard deviation of the true power distribution generated by wind data.

Figure 1 displays a Weibull probability distribution function (PDF) that describes the probabilistic behavior of the wind speed for a particular location-time. For analysis purposes, this curve is divided into four regions. Regions 1 and 4 represent times when wind speed is either too low to generate electricity or too or too high, which causes a safety shutdown of the wind generator. Hence, power in these regions is zero. In region 3, the wind is sufficient to produce full power; therefore, pitch control regulates this power. Finally, region 2 represents the region where the wind power generation truly varies.

These four regions can be translated into a wind power curve, as shown in Figure 2. This curve assumes that wind power linearly varies with the wind speed in region two, which is a valid approximation (Fu *et al.,* 2011). Based on the wind power curve, the active power supplied by the wind generator as a function of the wind speed is mathematically described by the following piecewise-defined function,

$$P_\omega^{Gen} = \begin{cases} 0 & \upsilon_\omega \leq \upsilon_{\omega,ci} \\ \alpha + \beta\upsilon_\omega & \upsilon_{\omega,ci} \leq \upsilon_\omega \leq \upsilon_{\omega,n} \\ P_\omega^{Gen,max} & \upsilon_{\omega,n} \leq \upsilon_\omega \leq \upsilon_{\omega,co} \\ 0 & \upsilon_\omega \geq \upsilon_{\omega,co} \end{cases} \quad (5)$$

where υ_ω is the wind speed, $\upsilon_{\omega,ci}$ is the cut-in wind speed below which no power is generated, $\upsilon_{\omega,co}$ is the cut-out wind speed above which no power is generated and $\upsilon_{\omega,n}$ stands for the full power wind speed. The maximum
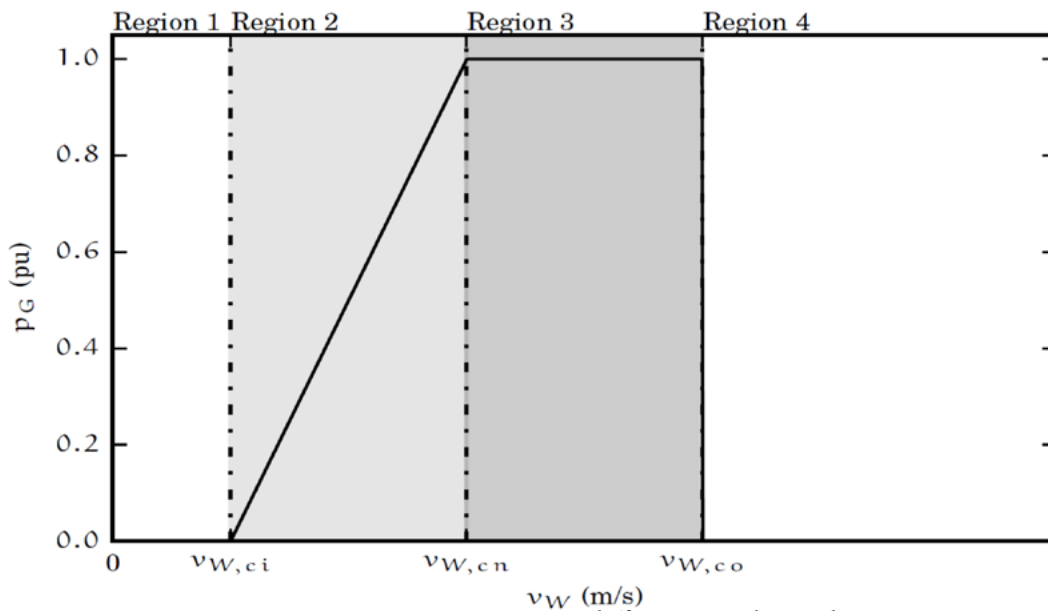

FIGURE 2. Output power at different wind speeds.

power generated by the wind farm is $p_\omega^{Gen,max}$. Lastly, constants α, and β are chosen to correspond with $\upsilon_{\omega,ci}$ and $\upsilon_{\omega,n}$ such that $\alpha + \beta\upsilon_{\omega,ci} = 0$ and $\alpha + \beta\upsilon_{\omega,n} = p_\omega^{Gen,max}$.

The core of the 5PEM is the approximation of the mixture of a discrete and continuous probability distribution by a discrete distribution with the whole probability mass concentrated at five points, as follows. The first point is determined from the tail areas under the Weibull distribution: regions 1 plus 4 producing zero power. Another point represents the full power region: region 3. Finally, the remaining three points represent the discretized version of region 2.

A. Algorithm

The variation of wind speed for a typical site is described by the analytical Weibull PDF function (Weibull, 1951) given by

$$f_{\upsilon_\omega}\left(\upsilon_\omega|\varphi,k\right) = \frac{k}{\varphi}\left(\frac{\upsilon_\omega}{\varphi}\right)^{k-1} e^{-\left(\frac{\upsilon_\omega}{\varphi}\right)^k} \tag{6}$$

where φ is the scale parameter, and k is the wind shape parameter. These constants may be determined from meteorological data at a specific site over a specified period. This work considers that these constants are known. For the reader interest, a few mathematical methods perform the Weibull curve fitting: (Jaramillo and Borja, 2004; Seguro and Lambert, 2000). On the other hand, the Weibull cumulative distribution function (CDF) is the area under the Weibull PDF and it is expressed as (Weibull, 1951)

$$F_{\upsilon_\omega}\left(\upsilon_\omega|\varphi,k\right) = \int_{-\infty}^{\upsilon_\omega} f_{\upsilon_\omega}\left(\upsilon_\omega|\varphi,k\right)d\upsilon_\omega = 1 - e^{\left(\frac{\upsilon_\omega}{\varphi}\right)^k} \tag{7}$$

Having (6) and (7) defined, we will consi-

der them to discretize the wind power curve into five points $\Phi_i = (P_i, C_i) \ \forall i \in \{1,...,5\}$, as follows. Note that each i-th point has its own wind power P_i and discrete probability C_i.

1) Point Φ_1

Point Φ_1 is associated with the probability that the wind power P_1 is equal to zero. This only happens when wind speed is very light such that the wind turbine cannot sustain any generation, or when wind speed is very high such that the wind turbine is safely turned off. Therefore, this point is calculated from the Weibull CDF as

$$P_1 = 0 \tag{8}$$

$$\begin{aligned} C_1 &= P_r\left(P_\omega^{Gen} = 0\right) = P_r\left(\upsilon_\omega \leq \upsilon_{\omega,ci}\right) + P_r\left(\upsilon_\omega \geq \upsilon_{\omega,co}\right) \\ &= F_{\upsilon_\omega}\left(\upsilon_{\omega,ci}|\varphi,k\right) + \left(1 - F_{\upsilon_\omega}\left(\upsilon_{\omega,co}|\varphi,k\right)\right) \end{aligned} \tag{9}$$

2) Point Φ_5

The fifth point represents the rated power operation and it is similarly determined by using the Weibull CDF,

$$P_5 = P_\omega^{Gen,max} \tag{10}$$

$$\begin{aligned} C_5 &= P_r\left(P_5 = P_\omega^{Gen,max}\right) = P_r\left(\upsilon_{\omega,n} \leq \upsilon_\omega \leq \upsilon_{\omega,co}\right) \\ &= \left(1 - F_{\upsilon_\omega}\left(\upsilon_{\omega,b}|\varphi,k\right)\right) - \left(1 - F_{\upsilon_\omega}\left(\upsilon_{\omega,co}|\varphi,k\right)\right) \end{aligned} \tag{11}$$

3) Points Φ_2, Φ_3 and Φ_4

The procedure to obtain these last three points involves an extended algebraic procedure out of the scope of this paper. For the reader interest, however, the complete procedure is shown in (Outcalt, 2009; Sandoval Perez, 2015). The wind power and discrete probability of each point is computed as follows,

$$P_2 = \bar{\mu} + \bar{\sigma} z_2,$$
$$C_2 = \rho_2 (1 - C_1 - C_5) \qquad , \qquad (12)$$

$$P_3 = \bar{\mu} + \bar{\sigma} z_3,$$
$$C_3 = \rho_3 (1 - C_1 - C_5) \qquad , \qquad (13)$$

$$P_4 = \bar{\mu} + \bar{\sigma} z_4,$$
$$C_4 = \rho_4 (1 - C_1 - C_5) \qquad , \qquad (14)$$

In these equations, $\bar{\mu}$ and $\bar{\sigma}$ correspond to the mean and variance values of the PDF of the wind power defined in between in Region 2, respectively:

$$\bar{\mu} = \int_0^{P_\omega^{Gen,max}} P_\omega^{Gen} \tilde{f}_{P_\omega^{Gen}} \left(P_\omega^{Gen} | \varphi, k \right) dP_\omega^{Gen}$$
$$\bar{\sigma} = \int_0^{P_\omega^{Gen,max}} \left(P_\omega^{Gen} - \bar{\mu} \right)^2 \tilde{f}_{P_\omega^{Gen}} \left(P_\omega^{Gen} | \varphi, k \right) dP_\omega^{Gen} \qquad (15)$$

where the continuous PDF, which is given by (16) (Sandoval Perez, 2015), has an area under the curve equal to one,

$$\tilde{f}_{P_\omega^{Gen}} \left(P_\omega^{Gen} | \varphi, k \right) = \frac{f_{v_\omega} \left(\left. \dfrac{P_\omega^{Gen} - \alpha}{\beta} \right| \varphi, k \right)}{(1 - C_1 - C_5) \beta} \qquad (16)$$

On the other hand, the standardized values of the wind power at each point are given by

$$z_2 = \frac{\lambda_3}{2} + \sqrt{\lambda_4 - \frac{3(\lambda_3)^2}{3}} \quad , \quad z_3 = 0 \quad , \quad z_4 = \frac{\lambda_3}{2} - \sqrt{\lambda_4 - \frac{3(\lambda_3)^2}{3}} \qquad (17)$$

where the standard central moments λ_3 and λ_4 of the random variable P_ω^{Gen} are given by

$$\lambda_j = \int_0^{P_\omega^{Gen,max}} \left(\frac{P_\omega^{Gen} - \bar{\mu}}{\bar{\sigma}} \right)^j \tilde{f}_{P_\omega^{Gen}} \left(P_\omega^{Gen} | \varphi, k \right) dP_\omega^{Gen} \quad , \quad j = 3, 4 \qquad (18)$$

Lastly, since the continuous distribution (16) in Region 2 is discretized into three points, the resulting discrete distribution has three discrete probabilities: ρ_2, ρ_3, and ρ_4 that also satisfies $\rho_2 + \rho_3 + \rho_4 = 1$. Hence, the values of these probabilities are given by (Sandoval Perez, 2015)

$$\rho_2 = -\frac{1}{z_2 (z_4 - z_2)} \, , \, \rho_3 = 1 - \rho_2 - \rho_4 \, , \, \rho_4 = -\frac{1}{z_4 (z_4 - z_2)} \qquad (19)$$

Based on the information reported above, Table 1 summarizes a 5PEM discrete power distribution of a wind generator.

Case Studies

The accuracy and efficiency of the 5PEM are tested by comparing its results with those obtained from the Monte Carlo simulation considering 10,000 samples. This number of simulations is high enough to guarantee the convergence of the MC method (Morales and Perez-Ruiz, 2007). Because of the high number of power flow simulations when using the MC method, a High-Performance Computing Cluster (HPCC) was used for the simulations. The probabilistic power flow was coded in the Python and C programming languages, with a multithreading approach to parallelizing several power flow simulations.

The effect of wind generation was incorporated by using simple synchronous generation dispatched at the active power obtained by either the 5PEM or the MC method. Each wind generator has voltage magnitude control capability; hence these wind generators are treated as *PV* buses (Ackermann, 2012).

The 5PEM approach is carried out through the following steps.

1. Estimate five discrete points for each wind farm by using the 5PEM algorithm.

2. Perform a caresian product with each five-point set; hence, the total combinations yield $n = 5^{n_{\omega f}}$ set of powers and the associated probabilities, where $n_{\omega f}$ is the total number of wind farms.

3. Run *n* power flows by considering each power combination.

TABLE 1. Five-point discrete distribution

Point	Φ_1	Φ_2	Φ_3	Φ_4	Φ_5
Wind farm power	0	P2	P3	P4	$p_\omega^{Gen,\max}$
5 PEM probability	C_1	C_2	C_3	C_4	C_5

(21)

The Monte Carlo simulations are performed as follows.

1. Generate 10,000 random wind speed values based on the Weibull distribution function of each wind farm. The random number generation is computed with a Mersenne Twister algorithm by using the built-in C language function. This number of MC simulations has demonstrated good results in other probabilistic power flows (Morales and Perez-Ruiz, 2007).

2. Evaluate this set of random wind speeds using (5); hence, a total of 10,000 wind powers are obtained.

3. Run power flows considering each power of the previous step.

Lastly, to provide an overview of the overall performance of the 5PEM, the following error indices are defined for each output random variable associated with the solution of the PPF:

$$\varepsilon_\mu^\chi = \left| \frac{\mu_{MC}^\chi - \mu_{5PEM}^\chi}{\mu_{MC}^\chi} \right| \times 100\%$$

(20)

$$\varepsilon_\sigma^\chi = \left| \frac{\sigma_{MC}^\chi - \sigma_{5PEM}^\chi}{\sigma_{MC}^\chi} \right| \times 100\%$$

(21)

where μ_{MC}^χ and σ_{MC}^χ are the mean and standard deviation associated with the results obtained by the Monte Carlo simulation, which are taken as reference values. Similarly, μ_{5PEM}^χ and σ_{5PEM}^χ are the mean and standard deviation from the 5PEM results. Finally, χ is any variable obtained from the PPF solution, which may refer to a nodal voltage at the i-th node, i.e., V_i and θ_i , the active and reactive power injected by the slack generator, P_{slack}^{Gen} and Q_{slack}^{Gen} , or the active and powers that flow through a transmission element connected between nodes i and j, i.e., P_{ij} and Q_{ij} .

The previous procedure is graphically picted in Figure 3, where we present a condensed flow-chart of the developed PPF.

A. Case A

The New England 39 bus system described in (Sandoval Perez, 2015) is modified to consider a WF with a 180 MW output rated power at bus 25. Wind farm data are shown in Table 2 as reported in (Jaramillo and Borja, 2004).

TABLE 2. Wind farm data.

WF	Bus	k	φ (m/s)	$\upsilon_{\omega,ci}$ (m/s)	$\upsilon_{\omega,n}$ (m/s)	$\upsilon_{\omega,co}$ (m/s)	$p_\omega^{Gen,\max}$ (pu)
I	25	1.768	11.861	3.57	13.4	25	1.8

Start

Read network data

¿Algorithm to use?

5PEM:

1. For each WF perform the 5PEM: $\Phi_i = (P_i, C_i) \in \Phi$, using (8)...(19), where $i = 1...5$

2. Create all the possible combinations: $n = \binom{\Phi}{5} = 5^{n_{wf}}$

Monte Carlo:

1. For each WF generate $n = 10,000$ random wind-speed values according to the Weibull PDF.

2. Compute:
   - Output power (P), with (5)
   - Set probability $C = \frac{1}{n}$

Parallel computation

$i=1$

For each WF:
- Update output power $P^{Gen} = P^{(i)}$

$i = i +1$

Solve the power flow problem by means of the NR method:

$\Delta P_i = P_i^{Gen} + P_{inj}^{Gen} - P_i^{Load} - V_i \sum_{j \in N} V_j \left[G_{ij} \cos(\theta_i - \theta_j) + B_{ij} \sin(\theta_i - \theta_j) \right] = 0, \ \forall i \in N^{PQ}$

$\Delta Q_i = Q_i^{Gen} + Q_{inj}^{Gen} - Q_i^{Load} - V_i \sum_{j \in N} V_j \left[G_{ij} \sin(\theta_i - \theta_j) - B_{ij} \cos(\theta_i - \theta_j) \right] = 0, \ \forall i \in N^{PQ}$

$\Delta P_i = P_i^{Gen} + P_{inj}^{Gen} - P_i^{Load} - V_i \sum_{j \in N} V_j \left[G_{ij} \cos(\theta_i - \theta_j) + B_{ij} \sin(\theta_i - \theta_j) \right] = 0, \ \forall i \in N^{PV}$

Save variables of interest.

(all points considered) $i=n$?

No

Yes

Compute mean (μ^x) and standard deviation (σ^x) values for each variable and each algorithm (5PEM and MC)

Start/Stop

FIGURE 3. PPF flow-chart.

By considering one wind farm connected at bus 25, $n_{\omega f} = 1$, five power flow smulations are performed, each one associated with each point of the discretized PDF as reported in Table 3. Table 4 shows the mean and standard deviation results for a selected set of variables, representing the general results obtained from both probabilistic approaches. As can be observed, the 5PEM provides good results compared with the Monte Carlo values, both for mean and standard deviation. By comparing the slack output power with both algorithms (5PEM and MC), the 5PEM represents the system's stochastic overall active power balance well.

Figure 4 and Figure 5 show the PDF and CDF of the active and reactive powers at the wind farm bus, respectively. It must be noted that the PDF for the 5PEM is concentrated at five points which are those obtained by the described scheme. On the other hand, the 5PEM CDF is similar to the CDF obtained from the MC simulations.

The computed five points can be appreciated in both Figure 4 and Figure 5: each estimated point represents or aggregates the MC results providing the same statistical distribution.

Finally, Figures 6 and 7 show distribution functions of the active and reactive powers of the slack generator, respectively. The PDF and CDF obtained using the 5PEM have similar values to those obtained by the MC approach.

B. Case B

A typical summer-day operating condition is studied in this section to assess the stochastic effect of different wind farms on the operation of a large scale interconnected power

TABLE 3. Calculated five-points for each wind farm

Wind farm	Φ_1	Φ_2	Φ_3	Φ_4	Φ_5
I	(0,0.137)	(1.578, 0.155)	(0.877, 0.280)	(0.206, 0.163)	(1.8, 0.265)

TABLE 4. Mean and standard deviation for Case A (selected values).

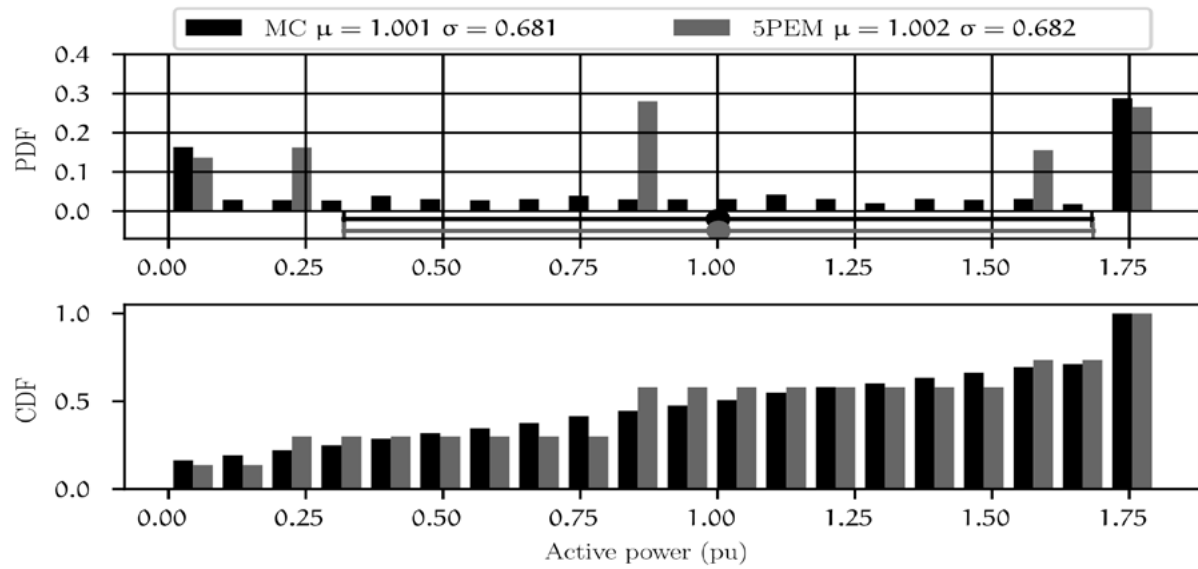| Case A		$P_{\omega,i}^{Gen}$	$Q_{\omega,i}^{Gen}$	P_{slack}^{Gen}	Q_{slack}^{Gen}	V_{16}	θ_{16}
Monte Carlo	μ	1.001	-6.335	5.320	2.168	1.007	-0.136
	σ	0.681	0.139	0.657	0.106	0.000	0.027
5PEM	μ	1.002	-6.335	-6.335	2.168	1.007	-0.136
	σ	0.682	0.139	0.139	0.106	0.000	0.027
Error (%)	ε_μ^χ	0.113	0.003	0.021	0.007	0.000	0.033
	ε_σ^χ	0.142	0.090	0.142	0.030	0.330	0.140

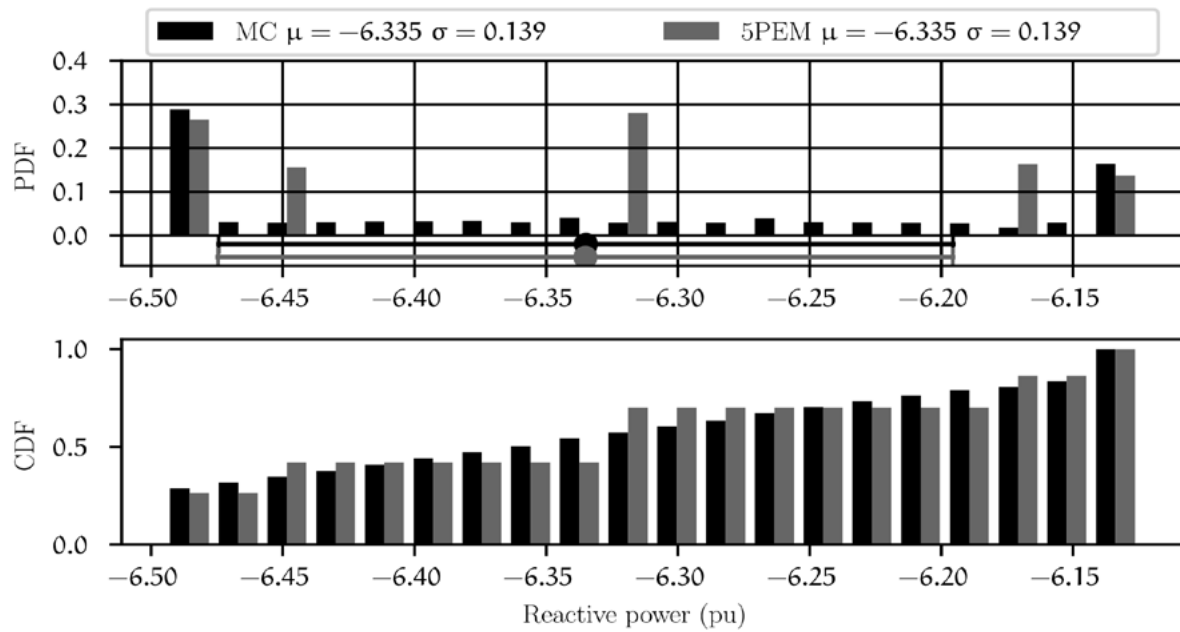FIGURE 4. PDF and CDF of the wind farm active power (Case A)·

Figure 5. PDF and CDF of the wind farm reactive power (Case A).

system. The network is composed of about 10,000 buses, 800 generators and 9000 transmission elements located in several control areas electrically interconnected for improving operating reliability and security.

The analysis is focused on the region with good wind resources, which must have an average wind speed of 7m/s or more (Jaramillo and Borja, 2004). These geographical characteristics have promoted more than 700 MW of installed capacity.

Two wind farms are modeled as stochastic generators to follow either the procedure of the 5PEM or a Monte Carlo simulation. The wind farm data used for the simulations are described in Table 5.

The generation of this region is mainly exported to the rest of the system by two power flow corridors referred to as "Tie-line 1" and "Tie-line 2" power flow corridors.

The PDF and CDF associated with the voltage magnitude and angle at node "HV01-400", which is the nearest high voltage bus to the zone of interest, are shown in 8 and 9, respectively. The results shown in both figures clearly show that the PDFs and CDFs obtained by the 5PEM and MC approaches compare well to each other.

On the other hand, an important part of the generation supplied from the southeast areas is collected at node "HV02-400".

The impact of wind power variability on the voltage at this node is shown in Figure 10 and Figure 11. Note that similar results are obtained using the 5PEM and MC methods.

Finally, the most important power flow corridors evaluated when new wind generation is incorporated in this region are the previously named "Tie-line 1" and "Tie-line 2" corridors. Each power flow corridor is made up of three high voltage (400 kV) transmission lines. Then, the impact of the wind power injection on both power flow corridors is depicted in Figure 12 and Figure 13.

A comparison of the results clearly shows that the PDFs and CDFs obtained by the 5PEM and MC approaches are in good agreement. Lastly, a comparison of the computational times required by the PPF based on the 5PEM and MC approach is given in Table 5. Note that the MC study needed approximately 7 minutes to complete 10,000 deterministic power flow solutions of the large-scale power system, while the time taken by 5PEM is about two seconds. Important detail is the usage of a parallel execution paradigm, in which case the MC power flow simulations were distributed along 64 cores. Each core solved the power flow, and the final solutions were then aggregated by a single core to consider the overall results.

Table 5. Windfarm data of the large -scale power system study

WF	k	φ (m/s)	$\upsilon_{\omega,ci}$ (m/s)	$\upsilon_{\omega,n}$ (m/s)	$\upsilon_{\omega,co}$ (m/s)	$p_{\omega}^{Gen,max}$ (MW)
I	2.1	9	4	15	25	240
II	2.12	8	4	15	25	240

Table 6. Time required for simulation studies

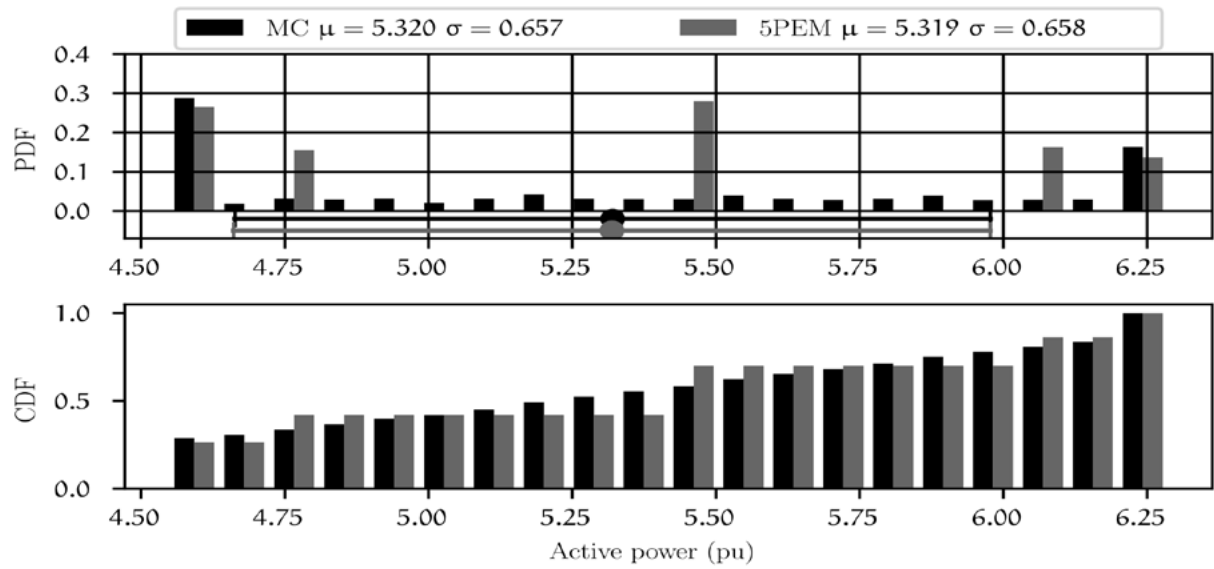| Case	5PEM	MC
Case A (New England test case)	0.089 s	22.375 s
Case B (Large-scale power system)	2.1 s	375 s

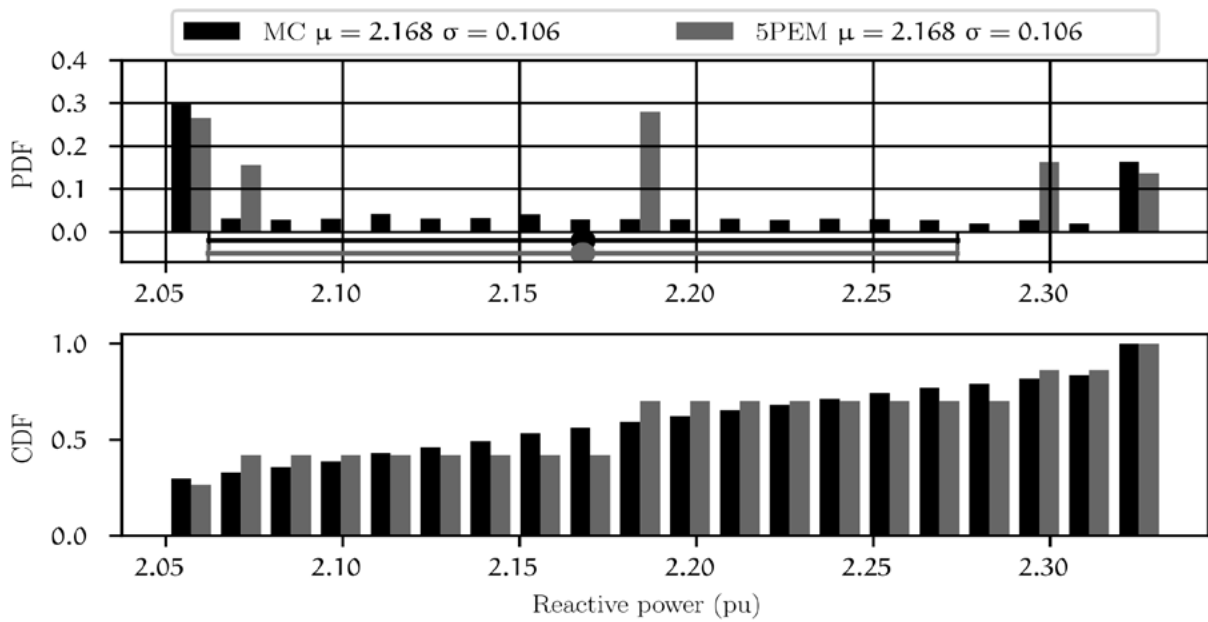Figure 6. PDF and CDF of slack active power (Case A).

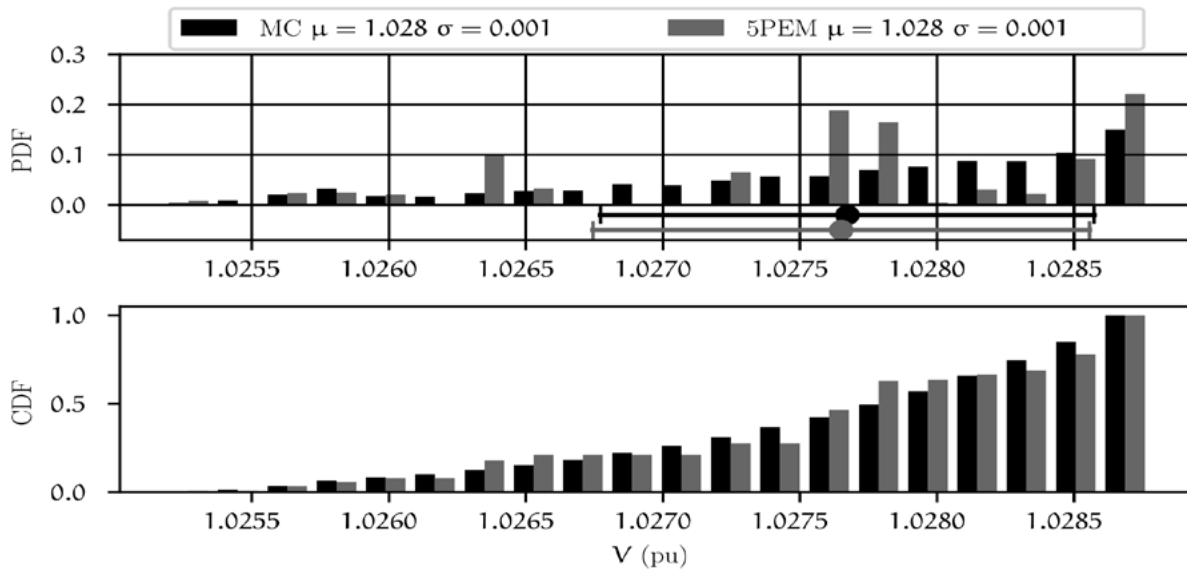Figure 7. PDF and CDF of the slack reactive power (Case A).

Figure 8. PDF and CDF of the voltage magnitude at bus HV01-400.
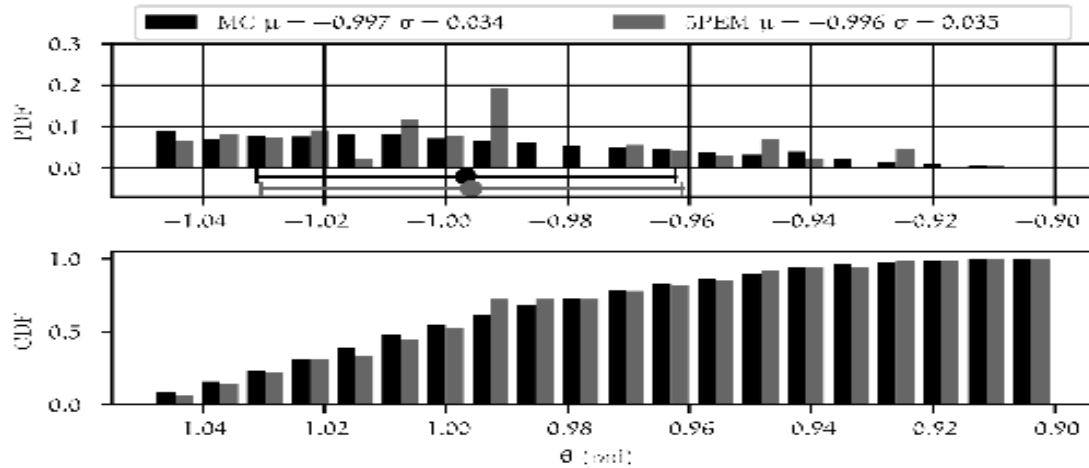

Figure 9. PDF and CDF of the voltage angle at bus HV01-400.
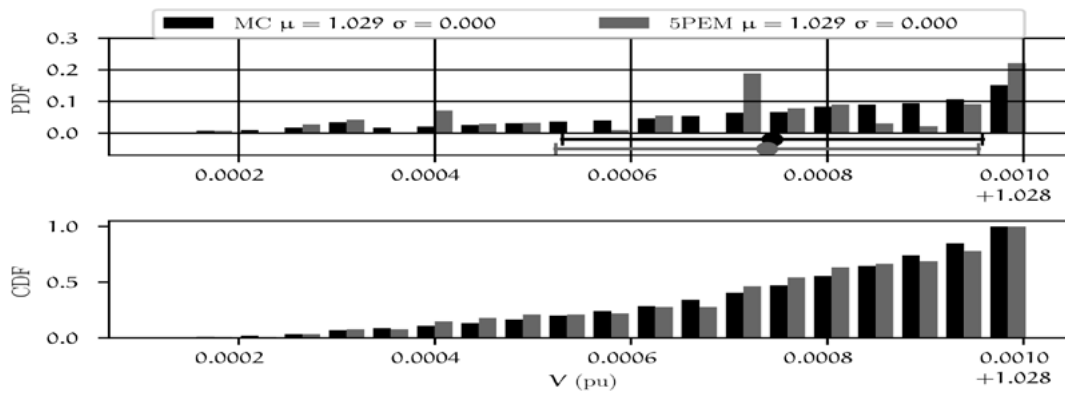

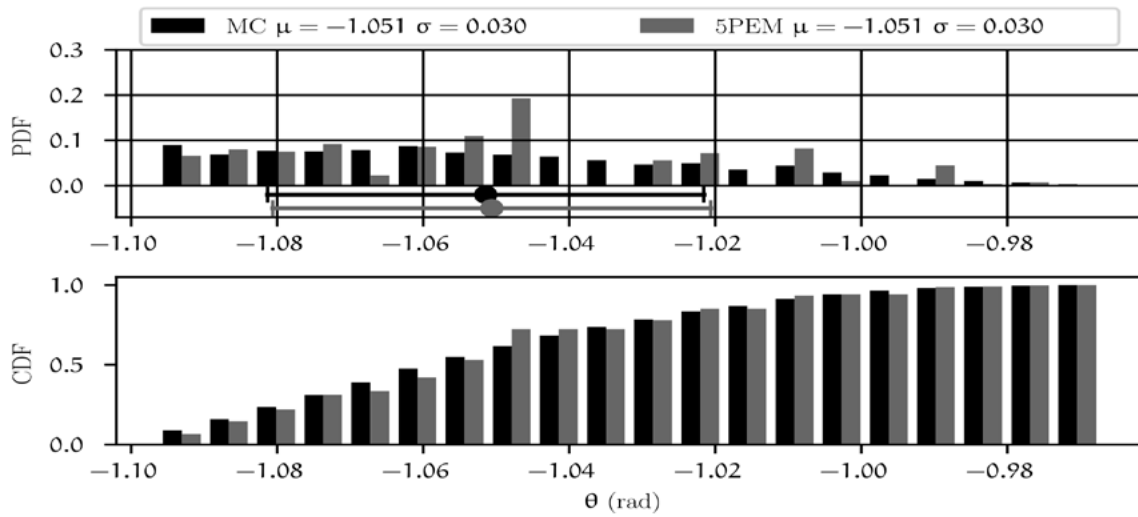Figure 10. PDF and CDF of the voltage magnitude at bus HV02-400.

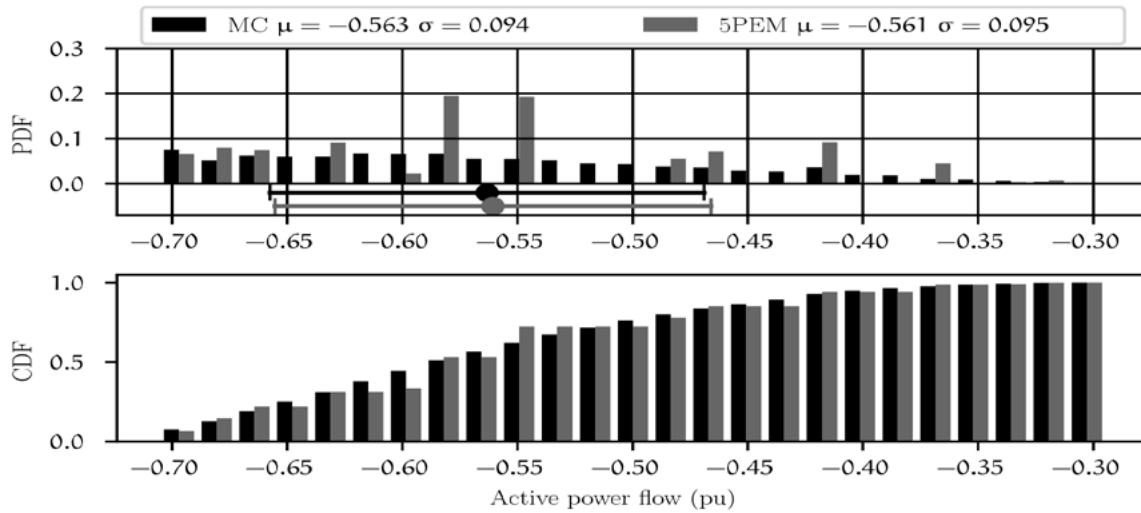Figure 11. PDF and CDF of the voltage angle at bus HV02-400.

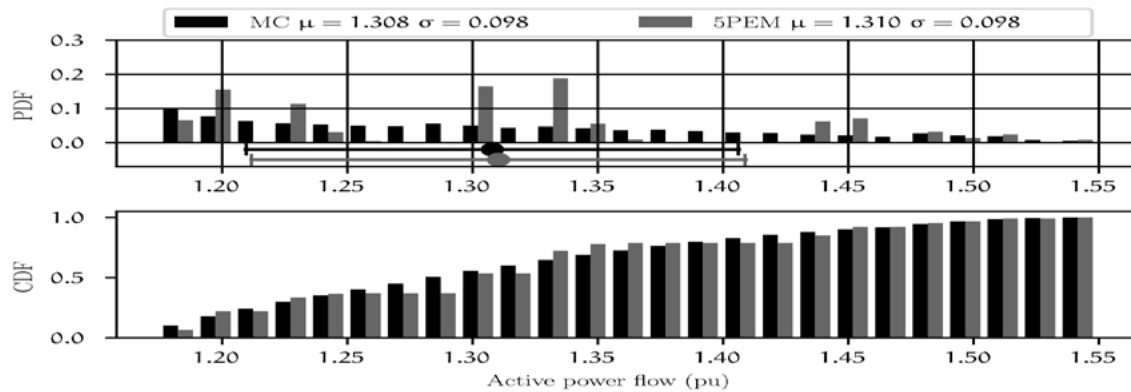Figure 12. PDF and CDF of power flow on "Tie-line 2" corridor.

Figure 13. PDF and CDF of power flow on "Tie-line 1" corridor.

Conclusion

This paper has reported an alternative to the traditional Monte Carlo method for handling stochastic phenomena in formulating the probabilistic power flow problem. In this sense, the 5PEM has been mathematically described to understand how a combination of discrete and continuous probability distribution functions can be concentrated in five points. Within this context, the 5PEM-based power flow formulation has been clearly described.

The numerical results show that the 5PEM-based power flow method is appropriate for evaluating the PDF, CDF, mean and standard deviations of nodal voltages and power flows in transmission grids. The overall precision of the results, compared with those obtained with the MC method, is very good for nodal voltages, i.e., <1% of relative error, and acceptable for power flows. Unlike the MC approach, however, the 5PEM provides good results, while keeping the computational burden low. Thus, including the 5PEM in the power flow problem provides an appropriate solution for the trade-off between the accuracy of the results and the efficiency of the computational procedure for large-scale power system problems.

Lastly, case studies demonstrate that 5PEM is a relevant tool for evaluating the integration of future WECS and accurately quantifying the transmission reinforcements or necessary adjustments to the transmission grid by considering stochastic scenarios.

References

Acha, E., Fuerte-Esquivel, C.R., Ambriz-Pérez, H., Angeles-Camacho, C., 2004. FACTS: Modelling and Simulation in Power Networks. *John Wiley & Sons.*

Ackermann, T. (Ed.), 2012. Wind power in power systems, 2nd ed. Wiley, Chichester, *West Sussex*; Hoboken, N.J.

Ahmed, S.D., Al-Ismail, F.S.M., Shafiullah, M., al-Sulaiman, F.A., El-Amin, I.M., 2020. Grid Integration Challenges of Wind Energy: *A Review. IEEE Access* 8, 10857–10878. https://doi.org/10.1109/ACCESS.2020.2964896

Ai, X., Wen, J., Wu, T., Lee, W.-J., 2012. A Discrete Point Estimate Method for Probabilistic Load Flow Based on the Measured Data of Wind Power 7

Chen, C., Wu, W., Zhang, B., Sun, H., 2015. Correlated probabilistic load flow using A point estimate method with Nataf Transformation. Int. J. Electr. *Power Energy Syst.* 65, 325–333.

Divya, K.C., Rao, P.S.N., 2006. Models for wind turbine generating systems and their application in load flow studies. *Electr. Power Syst. Res.* 76, 844–856. https://doi.org/10.1016/j.epsr.2005.10.012

Feijoo, A., 2009. On P Q Models for Asynchronous Wind Turbi *IEEE Trans. Power Syst.* 24, 1890–1891. https://doi.org/10.1109/TPWRS.2009.2030243

Feijoo, A.E., Cidras, J., 2000. Modeling of wind farms in the load flow analysis. *IEEE Trans.* Power Syst. 15, 110–115. https://doi.org/10.1109/59.852108

Fu, Q., Yu, D., Ghorai, J., 2011. Probabilistic load flow analysis for power systems with multi-correlated wind sources, in: 2011 IEEE Power and energy Society General Meeting. *Presented at the 2011 IEEE Power and Energy Society General Meeting,* pp. 1–6. https://doi.org/10.1109/PES.2011.603899

Gupta, N., 2016. Probabilistic load flow with detailed wind generator models considering correlated wind generation and correlated loads. *Renew Energy* 94, 96–105. https://doi.org/10.1016/j.renene.2016.03.030

GWEC, G.W.E., 2021. Global Wind Report 2021. Glob. Wind Energy Counc. Bruss. Belg.

IRENA, I., 2019. Future of wind: Deployment, investment, technology, grid integration and socio-economic aspects.

Jaramillo, O.A., Borja, M.A., 2004. Wind speed analysis in La Ventosa, Mexico: a bimodal probability distribution case. *Renew* Energy 29, 1613–1630.

HTTPS://DOI.ORG/10.1016/J.RENENE.2004.02.001

Mohammadi, M., Shayegani, A., Adaminejad, H., 2013. A new approach of point estimate method for probabilistic load flow. Int. J. Electr. *Power Energy Syst.* 51, 54–60. HTTPS://DOI.ORG/10.1016/J.IJEPES.2013.02.019

Morales, J.M., Perez-Ruiz, J., 2007. Point Estimate Schemes to Solve the Probabilistic Power Flow. IEEE Trans. *Power Syst.* 22, 1594–1601. HTTPS://DOI.ORG/10.1109/TPWRS.2007.907515

Outcalt, D.M., 2009. Probabilistic load flow for high wind penetrated power systems based on a five point estimation method. *The University of Wisconsin - Milwaukee.*

Padron, J.F.M., Lorenzo, A.E.F., 2010. Calculating Steady-State Operating Conditions for Doubly-Fed Induction Generator Wind Turbines. IEEE Trans. *Power Syst.* 25, 922–928. HTTPS://DOI.ORG/10.1109/TPWRS.2009.2036853

Restrepo Hernandez, J.F., 2011. Impact of wind energy on the operation of power systems. *McGill University.*

Sandoval Perez, U.F., 2015. Assessment of the Impact of Wind Power Generation on the Steady-State Operation of Power Systems. *Universidad Michoacana de San Nicolás de Hidalgo.*

Seguro, J.V., Lambert, T.W., 2000. Modern estimation of the parameters of the Weibull wind speed distribution for wind energy analysis. J. Wind Eng. Ind. *Aerodyn.* 85, 75–84. HTTPS://DOI.ORG/10.1016/S0167-6105(99)00122-1

Slootweg, J.G., Polinder, H., Kling, W.L., 2001. Initialization of wind turbine models in power system dynamics simulations, in: Power Tech Proceedings, 2001 IEEE Porto. Presented at the Power Tech Proceedings, 2001 *IEEE Porto,* p. 6 pp. vol.4-. HTTPS://DOI.ORG/10.1109/PTC.2001.964827

Su, C.-L., 2005. Probabilistic load-flow computation using point estimate method. IEEE Trans. *Power Syst.* 20, 1843–1851. HTTPS://DOI.ORG/10.1109/TPWRS.2005.857921

Weibull, W., 1951. A statistical distribution function of wide applicability. *J. Appl. Mech.* 18, 293–297.

Xiao, Q., He, Y., Chen, K., Yang, Y., Lu, Y., 2017. Point estimate method based on univariate dimension reduction model for probabilistic power flow computation. IET Gener.

Gener. Transm. Distrib. 11, 3522–3531. HTTPS://DOI.ORG/10.1049/IET-GTD.2017.0023

Zhu, X., Liu, C., Su, C., Liu, J., 2020. Learning-Based Probabilistic Power Flow Calculation Considering the Correlation Among Multiple Wind Farms. *IEEE Access* 8, 136782–136793. HTTPS://DOI.ORG/10.1109/ACCESS.2020.3011511